Influence of alpha-CH-->NH substitution in C8-CoA on the kinetics of association and dissociation of ligands with medium chain acyl-CoA dehydrogenase.

ARTICLE *in* BIOCHEMISTRY · NOVEMBER 2000

Impact Factor: 3.02 · Source: PubMed

3 AUTHORS, INCLUDING:

Karen Peterson
Mayo Foundation for Medical Education and …
20 PUBLICATIONS **199** CITATIONS
SEE PROFILE

Dharam Srivastava
North Dakota State University
81 PUBLICATIONS **1,358** CITATIONS
SEE PROFILE

Influence of α-CH→NH Substitution in C_8-CoA on the Kinetics of Association and Dissociation of Ligands with Medium Chain Acyl-CoA Dehydrogenase†

Karen M. Peterson, K. V. Gopalan, and D. K. Srivastava*

Department of Biochemistry and Molecular Biology, North Dakota State University, Fargo, North Dakota 58105

Received March 31, 2000; Revised Manuscript Received August 8, 2000

ABSTRACT: We previously reported that the kinetic profiles for the association and dissociation of functionally diverse C_8-CoA-ligands, viz., octanoyl-CoA (substrate), octenoyl-CoA (product), and octynoyl-CoA (inactivator) with medium chain acyl-CoA dehydrogenase (MCAD), were essentially identical, suggesting that the protein conformational changes played an essential role during ligand binding and/or catalysis [Peterson, K. L., Sergienko, E. E., Wu, Y., Kumar, N. R., Strauss, A. W., Oleson, A. E., Muhonen, W. W., Shabb, J. B., and Srivastava, D. K. (1995) *Biochemisry 34,* 14942−14953]. To ascertain the structural basis of the above similarity, we investigated the kinetics of association and dissociation of α-CH→NH-substituted C_8-CoA, namely, 2-azaoctanoyl-CoA, with the recombinant form of human liver MCAD. The rapid-scanning and single wavelength stopped-flow data for the binding of 2-azaoctanoyl-CoA to MCAD revealed that the overall interaction proceeds via two steps. The first (fast) step involves the formation of an enzyme−ligand collision complex (with a dissociation constant of K_c), followed by a slow isomerization step (with forward and reverse rate constants of k_f and k_r, respectively) with concomitant changes in the electronic structure of the enzyme-bound FAD. Since the latter step involves a concurrent change in the enzyme's tryptophan fluorescence, it is suggested that the isomerization step is coupled to the changes in the protein conformation. Although the overall binding affinity (K_d) of the enzyme−2-azaoctanoyl-CoA complex is similar to that of the enzyme−octenoyl-CoA complex, their microscopic equilibria within the collision and isomerized complexes show an opposite relationship. These results coupled with the isothermal titration microcalorimetric studies lead to the suggestion that the electrostatic interaction within the enzyme site phase modulates the microscopic steps, as well as their corresponding ground and transition states, during the course of the enzyme−ligand interaction.

Medium chain acyl-CoA dehydrogenase (MCAD)[1] catalyzes the insertion of α−β double bonds in fatty acyl-CoA substrates to produce their enoyl-CoA derivatives (for reviews, see *1*−*3*). The overall catalysis of the enzyme is comprised of the "reductive half-reaction", during which the oxidation of acyl-CoA to enoyl-CoA is coupled to the reduction of the enzyme-bound FAD to $FADH_2$, and the "oxidative half-reaction", during which the enzyme-bound $FADH_2$ is converted back to FAD, with concomitant transfer of the reducing equivalents to the external electron acceptors, such as electron transferring flavoprotein or ferricenium hexafluorophospate (*2, 3*; eq 1).Depending upon the type of acyl-CoA substrate, the enzyme catalysis is limited either by the forward rate constant of the reductive half-reaction or by the dissociation "off-rate" of the corresponding enoyl-CoA product (*4*−*7, 12*).

For the past several years, our research group has been interested in delineating the microscopic pathways for the binding/reactivity of different types of acyl-CoAs and their differently substituted/truncated analogues to MCAD (*6*−*8, 12*−*18*). In this pursuit, we noted that the binding/reactivity of shorter chain acyl-CoA substrates yielded somewhat different types of kinetic and thermodynamic profiles than those obtained for the binding of their corresponding enoyl-CoA products to the enzyme (*6, 13, 15, 19*). On the contrary, the binding/reactivity of medium chain acyl-CoAs, e.g., octanoyl-CoA (the physiological substrate of the enzyme), yielded precisely the same kinetic and thermodynamic profiles as those obtained for the binding of octenoyl-CoA (the physiological product of the enzyme; *8, 12)*. These similarities were also extended to the binding of octynoyl-CoA (a mechanism-based inactivator) to the enzyme (*8, 20*). The question arose as to how such chemically diverse processes yielded similar kinetic and thermodynamic characteristics. For example, in the case of octanoyl-CoA, the overall process involves "chemistry" (i.e., proton and hydride transfer), but in the cases of octenoyl-CoA and 2-octynoyl-CoA, the overall process simply involves the changes in the electronic structure of the enzyme-bound FAD. If the kinetic profiles and the overall binding constants of all these ligands are the same, it implies that the ground and transition state energies of all the corresponding steps must be the same (*7*−*8, 12*). This inference initially appeared to be surprising,

† This work was supported by National Science Foundation Grant MCB-9904416.

* To whom correspondence should be addressed at the Department of Biochemistry and Molecular Biology, North Dakota State University, Fargo, ND 58105. Tel: (701) 231-7831; Fax: (701) 231-9657; Email: DK_Srivastava@ndsu.nodak.edu.

[1] Abbreviations: MCAD, medium chain acyl-CoA dehydrogenase; FAD, flavin adenine dinucleotide; $FcPF_6$, ferricenium hexafluorophosphate; ETF, electron transferring flavoprotein; RSSF, rapid-scanning stopped-flow; SWSF, single wavelength stopped-flow; $\Delta G°$, standard free energy change; $\Delta H°$, standard enthalpy change; $\Delta S°$, standard entropy change; CoA, coenzyme A; Aza-CoA, 2-azaoctanoyl-CoA; Oce-CoA, 2-octenoyl-CoA.

10.1021/bi000733w CCC: $19.00
Published on Web 09/16/2000

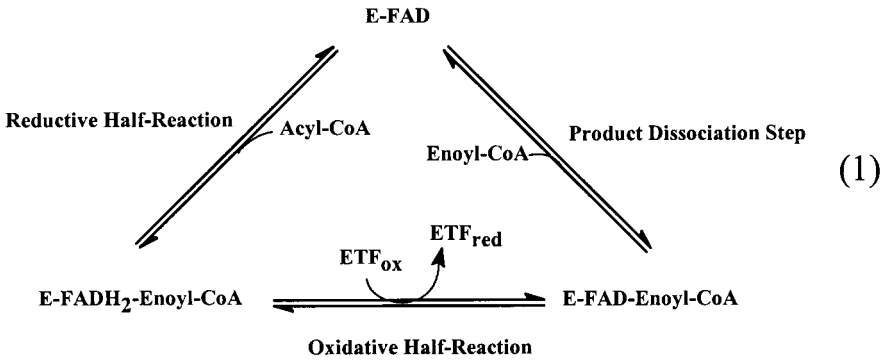

Scheme 1

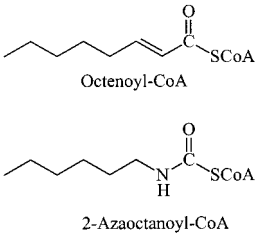

but it could be explained on consideration that a common denominator in the overall binding/reactivity process, e.g., the protein conformational change, was the driving force for altering the ligand structures (i.e., "chemistry" and/or the "electronic structures" of FAD and CoA-ligands; *7, 12*).

The above hypothesis prompted us to investigate the role of slightly altered (but of an identical chain length) ligand on the kinetic and thermodynamic profiles of the enzyme−ligand interactions. In this endeavor, we noted that the substitution of an α-methylene group by an amine group in octanoyl-CoA generates a redox inactive ligand, viz., 2-aza-octanoyl-CoA (*21*), which induces a different type of electronic structural change in the enzyme-bound FAD, as compared to octenoyl-CoA (Scheme 1).

We considered that detailed kinetic and thermodynamic studies for the binding of 2-azaoctanoyl-CoA and octenoyl-CoA would throw light on the coupling between the protein conformational changes and the changes in the ligand structures. Such studies deemed to be further important since 2-azaoctanoyl-CoA had been argued to serve as the transition state analogue of the enzyme (*22*).

The X-ray crystallographic structures of both pig liver and recombinant human liver MCAD's in the absence and presence of octenoyl-CoA have been solved to atomic resolutions (*23*−*25*). The structural data reveal that octenoyl-CoA is bound in a somewhat "zigzagged " pocket, and is primarily surrounded by the side chains of the hydrophobic amino acid residues. Except for the presence of a few polar side chains around the coenzyme-A binding region, the carboxyl group of Glu-376 is pointed toward the α-carbon of C_8-CoA (and just poised to abstract the α or γ proton from acyl-CoA substrates), and the carbonyl oxygen of acyl/enoyl-CoA is hydrogen bonded to the 2′-ribityl hydroxyl group of FAD as well as to the amide nitrogen of Glu-376 (*24*; Figure 1). The latter interactions have been implicated in the polarization of the carbonyl group of the acyl/enoyl-CoA species, which has been demonstrated to be responsible for the stabilization of the ground and transition states of the enzyme during catalysis (*9*). In light of these structural

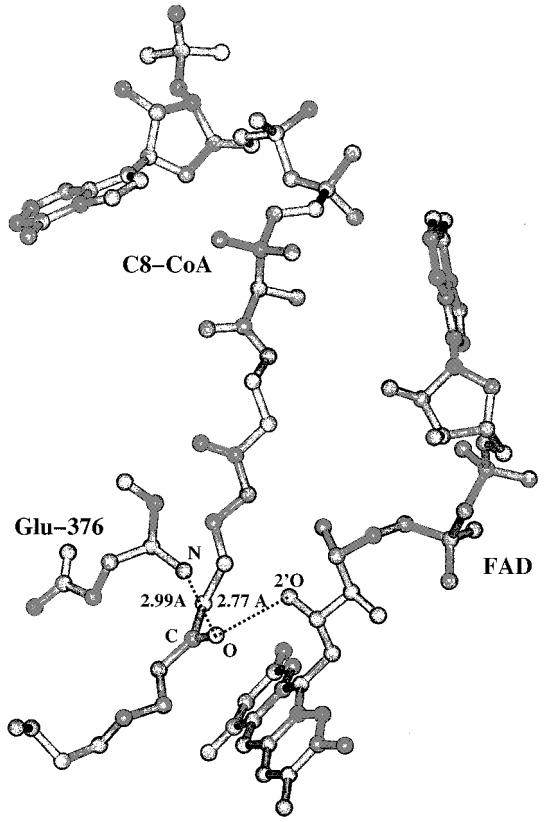

FIGURE 1: Spatial relationship among the enzyme-bound FAD, octenoyl-CoA (C_8-CoA), and Glu-376 residue within the active site of pig liver medium chain acyl-CoA dehydrogenase. The distances between the carbonyl oxygen of C_8-CoA and the 2′-ribityl oxygen of FAD and the amide nitrogen of Glu-376 are shown by the broken lines.

features, as well as the known spectroscopic properties of the enzyme−ligand complexes, we undertook detailed comparative studies for the binding of octenoyl-CoA and 2-aza-octanoyl-CoA to recombinant human liver MCAD via the transient kinetic and microcalorimetric methods.

MATERIALS AND METHODS

Materials. Coenzyme A was purchased from Life Science Resources. *trans*-2-Octenoic acid was purchased from Pfaltz and Bauer, and *n*-hexyl isocyanate was purchased from Acros. All other reagents were of analytical grade.

Methods. Unless otherwise stated, all experiments were performed in 50 mM potassium phosphate, pH 7.6, containing 10% glycerol and 0.3 mM EDTA (referred to as the standard buffer throughout the manuscript). Recombinant human liver MCAD was expressed and purified according

to Peterson et al. (*8*), and routinely assayed by monitoring the reduction of ferricenium hexafluorophosphate ($FcPF_6$) at 300 nm ($\epsilon = 4.3$ mM^{-1} cm^{-1}; *26*) in a reaction mixture containing 100 μM octanoyl-CoA and 350 μM $FcPF_6$. The purified enzyme preparation had an A_{280}/A_{450} ratio of about 5. The extinction coefficient of the enzyme-bound FAD was taken to be 15.4 mM^{-1} cm^{-1} at 446 nm (*27*)

Octenoyl-CoA was prepared by the mixed anhydride method of Bernhert and Sprecher (*28*) and purified on a C_{18} reverse-phase HPLC column, equilibrated with 20 mM potassium phosphate, pH 7.0, as described by Kumar and Srivastava (*7*). The ligand, 2-azaoctanoyl-CoA, was prepared essentially as described by Trievel et al. (*21*). A solution of *n*-hexyl isocyanate, dissolved in THF, was added to a solution of coenzyme A (in 0.25 M $NaHCO_3$) under a nitrogen stream. The reaction mixture was stirred under nitrogen for 30 min, after which the pH was adjusted to 5.5 with acetic acid. The resultant product was purified on a C_{18} reverse-phase HPLC column, equilibrated with 20 mM ammonium acetate, pH 5.5, as described above. All CoA derivatives were stored as lyophilized powders at −20 °C. The extinction coefficients of octenoyl-CoA and 2-azaoctanoyl-CoA were taken to be 20.4 mM^{-1} cm^{-1} at 258 nm and 16.0 mM^{-1} cm^{-1}at 260 nm, respectively (*7, 21*).

Rapid-Scanning Stopped-Flow (RSSF) Kinetic Studies. The RSSF kinetic studies were performed on an Applied Photophysics SX-18MV stopped-flow system, equipped with a photodiode array (PD-1) assembly. A 150 W arc Xenon lamp was used as the light source. The mixing of reagents and data acquisitions were automated via the software developed by Applied Photophysics.

Steady-State Spectrofluorometric Studies. The excitation and emission spectra of the enzyme in the absence and presence of CoA-ligands were performed on a Perkin-Elmer LS-50B Luminescence Spectrometer. For emission spectra of the enzyme's tryptophan, the excitation wavelength was fixed at 295 nm, and a 350 nm cutoff filter was placed in the emission path.

Transient Kinetic Experiments. Single wavelength transient kinetic experiments were performed on an Applied Photophysics SX-18 MV stopped-flow system (optical path length 10 mm, dead time 1.3−1.5 ms). The stopped flow was configured in a single mixing mode, in which the contents of both syringes A and B were diluted by 50%. The stopped-flow system had the capability to acquire the time course of the fluorescence changes by configuring the photomultiplier tube at the right angle of the incident light. The excitation wavelength (295 nm) was selected by the monochromator. A cutoff filter of 335 nm was placed prior to the entrance of light to the photomultiplier tube.

The rate constants for the association of the ligands to the enzyme were determined by mixing the above species via the stopped-flow syringes [under pseudo-first-order conditions ([E−FAD] ≪ [ligand])], and monitoring the time-dependent absorbance changes at specific wavelengths. The rate constants for the dissociation of ligands from the enzyme site were determined by the acetoacetyl-CoA displacement method as described by Johnson et al. (*15*).

All the transient kinetic experiments were performed at least in triplicate, and the resultant kinetic traces were averaged prior to analyses of the experimental data by the software developed by Applied Photophysics.

Spectrophotometric Titrations for the Binding of Ligands to MCAD. Spectrophotometric titrations were performed either on a Perkin-Elmer Lambda-3B or on a Beckman 7400 diode array spectrophotometer. The difference spectra of the enzyme−ligand complexes were generated by subtracting the spectra of the individual components from their mixtures (after dilution corrections). The binding isotherms for the enzyme−ligand interactions were constructed by titration of the enzyme with 2-azaoctanoyl-CoA and octenoyl-CoA at 438 and 442 nm, respectively. The dissociation constants and the overall amplitude of the absorbance changes were obtained by analyzing the experimental data by a complete solution of the quadratic equation (describing enzyme−ligand interaction) as elaborated by Qin and Srivastava (*29*).

Isothermal Titration Microcalorimetric Studies. Isothermal titration microcalorimetric experiments were performed on an MCS isothermal titration microcalorimeter from Microcal Inc. as described by Srivastava et al. (*10*). The sample cell was filled with 1.8 mL (1.36 mL effective volume) of the buffer (control) or the enzyme solution (experiment). The injector was filled with 250 μL of the appropriate ligand. The titration was initiated by a preliminary first injection of 1 μL followed by 59 injections of 4 μL each. During the experiment, the enzyme solution was stirred at a constant rate of 400 rpm.

All calorimetric data were presented after correction for the background. Since the titration produced small turbidity in the enzyme solution, the background heat was somewhat larger than that obtained for dilution of the ligand in the buffer medium. Thus, the heat produced at the end of the titration, where the enzyme was saturated with the ligand, was taken as a measure of the background heat. The experimental data were analyzed according to Wiseman et al. (*46*).

The data analysis produced three parameters, viz., stoichiometry (n), the association constant (K_a), and the standard enthalpy change ($\Delta H°$) for the binding of the ligand to MCAD. The standard free energy change ($\Delta G°$) for the binding was calculated according to the relationship: $\Delta G° = -RT \ln K_a$. Given the magnitudes of $\Delta G°$ and $\Delta H°$, the standard entropy change ($T\Delta S°$) for the binding process was calculated according to the standard thermodynamic equation: $\Delta G° = \Delta H° - T\Delta S°$.

RESULTS

To ascertain the nature and magnitude of the electronic structural changes during the (transient) course of binding of 2-azaoctanoyl-CoA to the oxidized form of the enzyme (MCAD−FAD), we employed the rapid-scanning stopped-flow (RSSF) system as described under Materials and Methods. Figure 2 shows the RSSF data for the mixing of 40 μM MCAD with 400 μM 2-azaoctanoyl-CoA (premixing concentrations), in the standard phosphate buffer, pH 7.6, at 5 °C, via the stopped-flow syringes. Note that the binding of 2-azaoctanoyl-CoA to MCAD results in an increase in absorbance at 390 and 490 nm, and a decrease in absorbance at 347 and 438 nm, respectively. These spectral changes become more pronounced in the difference spectra, which are generated by subtracting the first spectrum from the subsequent (time-dependent) spectra (Figure 2B). The data of Figure 2A,B reveal that the overall spectral changes conform to the isosbestic points at 313, 373, 399, 467, and

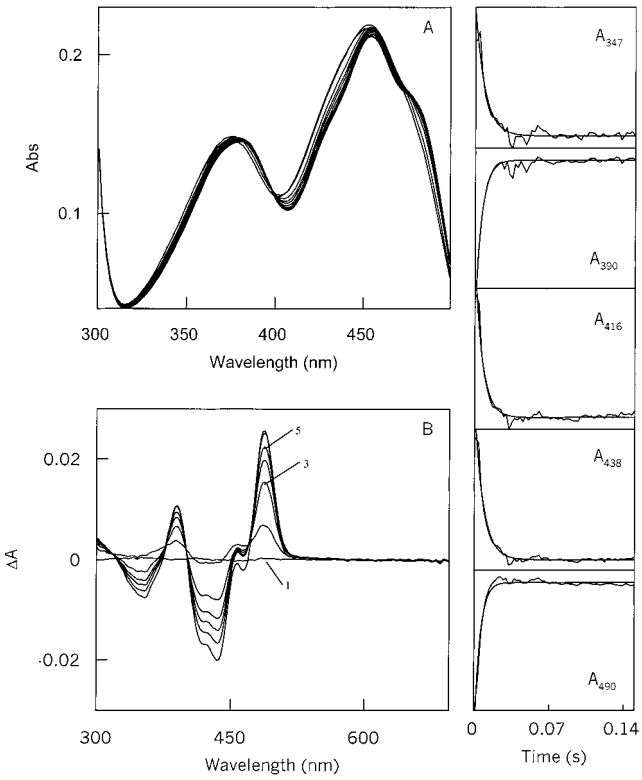

FIGURE 2: Rapid-scanning stopped-flow (RSSF) spectral data for the binding of 2-azaoctanoyl-CoA to MCAD. The spectral acquisition was performed in 50 mM potassium phosphate buffer, pH 7.6, containing 0.3 mM EDTA and 10% glycerol, at 5 °C. Panel A shows the spectral changes upon mixing 40 μM MCAD with 400 μM 2-azaoctanoyl-CoA (the premixing concentrations) via the stopped-flow syringes. Panel B shows the difference spectra, obtained by subtracting the first spectrum from the subsequent spectra of the enzyme−ligand complex. For clarity, only a selected set of the spectral data is shown in sequence of increasing time interval (e.g., 1, 3, 5). The right side panels show the time slices of the spectral changes at selected wavelengths. The solid smooth lines are the best fit of the experimental data according to the single-exponential rate equation. The rate constants of the kinetic traces at different wavelengths are as follows: 347 nm, 114 s^{-1}; 390 nm, 162 s^{-1}; 416 nm, 142 s^{-1}; 438 nm, 123 s^{-1}; 490 nm, 196 s^{-1}.

499 nm. As observed with other CoA-ligands (*6*, *8*, *15*), no spectral changes occurred within the dead-time of our RSSF system upon initial binding of 2-azaoctanoyl-CoA to the enzyme (data not shown).

As noted herein, as well as by others, a prolonged incubation of 2-azaoctanoyl-CoA with the enzyme results in a further decrease in absorption at 450 nm (*22*−*23*). However, the latter effect is not due to the reduction of the enzyme-bound FAD, since it occurs both under anaerobic as well as under aerobic conditions, and the "apparently" bleached enzyme is not oxidizable upon exposure to oxygen (data not shown). Since all the transient kinetic experiments reported herein have been performed prior to the onset of the slow spectral changes (as noted above), our overall conclusion remains unaffected by the latter event.

The side panels of Figure 2 are the time slices of the RSSF data at selected wavelength regions. The solid smooth lines are the best fit of the experimental data according to the single-exponential rate equation, with the rate constants ranging from 114 to 187 s^{-1}.

Association and Dissociation Kinetics. Although the time slices of the RSSF data at different wavelength regions (such as presented in Figure 2) provide a reasonable (albeit qualitative) measure of the association parameters of the enzyme−ligand complexes, the latter are quantitatively determined by performing the single wavelength stopped-flow (SWSF) experiments. Figure 3A shows a representative SWSF trace (monitored at 438 nm) upon mixing 40 μM enzyme with 400 μM 2-azaoctanoyl-CoA (premixing concentrations), in the standard phosphate buffer, pH 7.6, at 5 °C. The solid

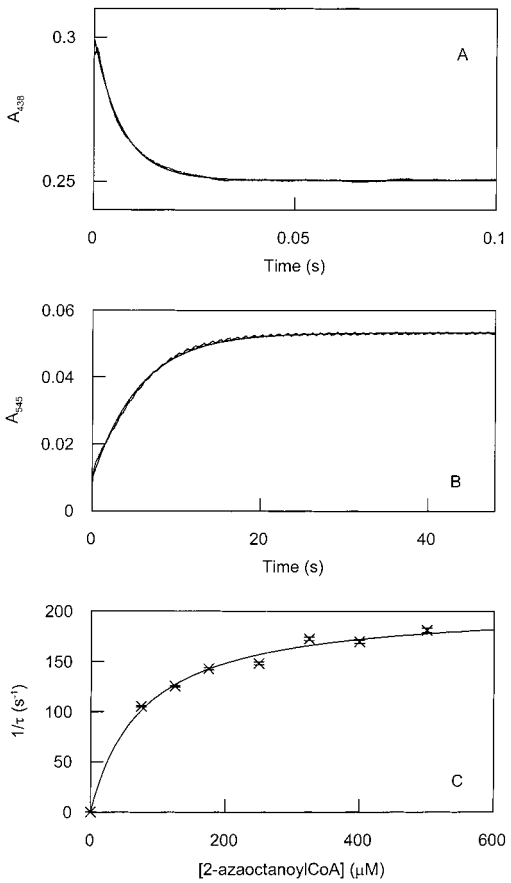

FIGURE 3: Single wavelength stopped-flow (SWSF) kinetic data for the association and dissociation of 2-azaoctanoyl-CoA with MCAD. The other experimental conditions are the same as in Figure 2. Panel A shows a representative stopped-flow trace for the association of 40 μM MCAD with 400 μM 2-azaoctanoyl-CoA (premixing concentrations) at 438 nm. The solid smooth line is the best fit of the data according to the single-exponential rate equation with a relaxation rate constant ($1/\tau$) of 143 ± 2 s^{-1} and an amplitude of 0.05 absorption unit. Panel B shows a stopped-flow trace for the dissociation of 2-azaoctanoyl-CoA from the enzyme site. The above trace was obtained by mixing 40 μM enzyme + 40 μM 2-azaoctanoyl-CoA (syringe 1; premixing concentrations) with 2 mM acetoacetyl-CoA (syringe 2; premixing concentration), and measuring the absorption changes at 545 nm. The solid smooth line is the best fit of the experimental data according to the single-exponential rate equation with a rate of 0.18 ± 0.001 s^{-1}, and amplitude of 0.044 absorption unit. Panel C shows the 2-azaoctanoyl-CoA concentration-dependence of the relaxation rate constant ($1/\tau$) for the enzyme−ligand association, measured at 438 nm. The solid smooth line is the best fit of the experimental data for the hyperbolic dependence of $1/\tau$ on 2-azaoctanoyl-CoA concentration with offset, with the magnitudes of the relaxation rate constants at zero ($1/\tau_{min}$) and saturating ($1/\tau_{max}$) concentrations of 2-azaoctanoyl-CoA, and the concentration of 2-azaoctanoyl-CoA required for achieving the half of the total changes in the relaxation rate constants (K_c) being equal to 0.18 ± 0.001 s^{-1}, 205 ± 10 s^{-1}, and 76.6 ± 7 μM, respectively. The data point at zero concentration of 2-azaoctanoyl-CoA has been taken from the dissociation "off-rate" measurement of the ligand from panel B.

smooth line is the best fit of the experimental data for the rate constant of 143 ± 2 s^{-1}. The latter value falls in the range of the (qualitative) rate constants derived from the RSSF data of Figure 2 (see above).

It should be mentioned that we could not reliably perform the RSSF studies for the binding of octenoyl-CoA to MCAD even at 5 °C due to its higher association rate constant. However, in their detailed single wavelength stopped-flow studies, Peterson et al. (*8*) reported that the binding of octenoyl-CoA to the enzyme (in the standard phosphate buffer, at 5 °C, but without glycerol) was consistent with the biphasic kinetic profiles, with fast and slow relaxation rate constants of 676 ± 72 and 38 ± 6 s^{-1}, respectively. These kinetic data (in conjunction with the numerical simulation studies) were previously explained to be consistent with the formation of the enzyme−ligand collision complex, followed by the two sequential isomerization steps, of which the first step had an equilibrium constant near unity (*8*, *12*). However, subsequent studies on the effect of deletion of the 3′-phosphate moiety of coenzyme A (*16*) and the temperature-dependent analysis of the relaxation rate constants (*30*), as well as the tryptophan fluorescence data (see Figure 6), led to the suggestion that the kinetic mechanism of the enzyme−octenoyl-CoA interaction could be reliably explained without involving the slower relaxation phase. Besides simplifying the kinetic complexity, the above stratagem facilitated a straightforward comparison between the microscopic parameters for the binding of octenoyl-CoA and 2-azaoctanoyl-CoA to the enzyme (see below). From a casual comparison between the single-exponential rate constant for the binding of 2-azaoctanoyl-CoA to the enzyme (Figure 3A) with the fast rate constant for the binding of octenoyl-CoA to the enzyme (*8*), it is evident that the former is about 5-fold slower than the latter. Hence, in qualitative terms, the α-CH→NH substitution in C_8-CoA impairs the rate of enzyme−ligand association.

Figure 3B shows the stopped-flow kinetic trace for the dissociation of 2-azaoctanoyl-CoA from the enzyme site. This experiment was performed by competitive displacement of the enzyme-bound ligand in the presence of a high and saturating concentration of acetoacetyl-CoA, as elaborated by Johnson et al. (*15*). As per this method, an enzyme−ligand ([enzyme] ≈ [ligand]) complex is mixed with a high (and saturating) concentration of acetoacetyl-CoA via the stopped-flow syringes, and the time course for the increase in absorption at 545 nm (due to the formation of the enzyme−acetoacetyl-CoA complex) is monitored (*12*, *15*). Since the formation of the enzyme−acetoacetyl-CoA complex occurs following the dissociation of the ligand, the kinetic profile serves as a measure of the dissociation "off-rate" constant of the enzyme−ligand complex (*12*). The kinetic trace of Figure 3B shows an increase in absorption at 545 nm upon mixing a solution of 40 μM enzyme + 40 μM 2-azaoctanoyl-CoA with 2 mM acetoacetyl-CoA (premixing concentrations) via the stopped-flow syringes. The solid smooth line is the best fit of the experimental data for the dissociation "off-rate" of 2-azaoctanoyl-CoA which is 0.18 ± 0.001 s^{-1}. When an identical experiment was performed for the dissociation of octenoyl-CoA from the enzyme−octenoyl-CoA complex, a dissociation "off-rate" of 1.0 ± 0.01 s^{-1} was discerned (data not shown). Hence, the dissociation "off-rate" of 2-azaoctanoyl-CoA is about 5-fold lower than that of octenoyl-CoA from the corresponding enzyme−ligand complex. Clearly, like the association rate constant, the αCH→NH substitution in C_8-CoA impairs the dissociation rate constant of the ligand by more or less the same magnitude. These results lead to the suggestion that the αCH→NH substitution impairs the rapidity of binding of the C_8-CoA-ligand to the enzyme, but once the ligand is bound, its dissociation is also impaired.

To determine the sequence of steps leading to the binding of 2-azaoctanoyl-CoA to the enzyme, we determined the magnitudes of the association rate constant, i.e., the relaxation rate constant ($1/\tau$), as a function of 2-azaoctanoyl-CoA under the pseudo-first-order condition ([enzyme] ≪ [ligand]). Figure 3C shows the hyperbolic dependence of $1/\tau$ on 2-azaoctanoyl-CoA concentration. The solid smooth line is the best fit of the experimental data for the hyperbolic dependence of $1/\tau$ on 2-azaoctanoyl-CoA, with an offset (i.e., the zero ligand concentration point). It should be mentioned that for accuracy the latter value was taken from the dissociation "off-rate" measurement of the enzyme−2-azaoctanoyl-CoA complex (Figure 3B). The analysis of the experimental data of Figure 3C yields the magnitudes of $1/\tau_{max}$ (the rate constant at a saturating concentration of 2-azaoctanoyl-CoA), $1/\tau_{min}$ (the rate constant at zero concentration of 2-azaoctanoyl-CoA, which is equal to the dissociation "off-rate" of the enzyme−ligand complex), and K_c (the concentration of 2-azaoctanoyl-CoA required to achieve half of the maximum saturation) to be 205 ± 10 s^{-1}, 0.18 ± 0.001, and 76.6 ± 7 μM, respectively.

Changes in Protein Conformation upon Ligand Binding. Although the evidence for the isomerization of the enzyme−ligand complexes (see eq 2) has been suggestive of the protein conformational change, there has been no independent experimental data to support such a possibility. This is particularly so since the signal for interaction between the enzyme and ligand has been primarily derived from the electronic structural changes of the enzyme-bound FAD, and not from the signal(s) associated with the protein structure (*8*, *12*, *15*, *32*). In pursuit of probing the latter signal, we discovered that the fluorescence emission spectrum of the enzyme in the tryptophan region is quenched upon binding of the CoA-ligands. By utilizing the fluorescence signal, we performed the transient kinetics for the association of 2-azaoctanoyl-CoA and octenoyl-CoA with the enzyme, to probe the similarity in the microscopic pathways for the enzyme−ligand interactions as well as to determine the intrinsic microscopic parameters (see below).

Figure 4 shows the fluorescence emission spectra of the enzyme (λ_{ex} = 295 nm) in the absence (trace 1) and presence of 5 μM 2-azaoctanoyl-CoA (trace 2) or 5 μM octenoyl-CoA (trace 3). Note that the fluorescence emission spectrum of the enzyme is slightly blue shifted, and quenched by 6−10% upon binding with the above ligands, respectively, suggesting that the microenvironments of the enzyme-resident tryptophan residues are altered upon interaction with the above ligands.

By utilizing the fluorescence emission signals of Figure 4, we performed the transient kinetic studies for the binding of 2-azaoctanoyl-CoA and octenoyl-CoA to the enzyme. Figure 5A shows the time-dependent decrease in the enzyme's tryptophan fluorescence (λ_{ex} = 295 nm, cutoff filter = 335 nm) upon mixing (premixing concentrations) of 8 μM

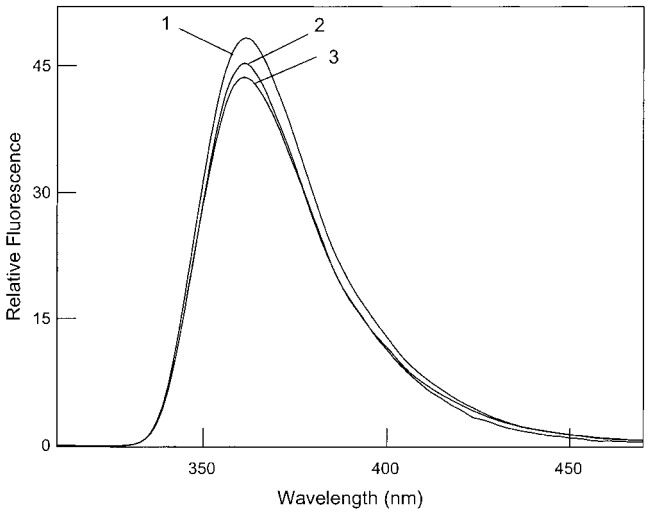

FIGURE 4: Tryptophan fluorescence emission spectra of MCAD in the absence and presence of 2-azaoctanoyl-CoA and octenoyl-CoA. The emission spectra were obtained following excitation at 295 nm, and using a cutoff filter at 350 nm. The concentrations of different components and the corresponding fluorescence spectra are as follows: [MCAD] = 1 μM (trace 1), [MCAD] = 1 μM + [2-azaoctanoylCoA] = 5 μM (trace 2), and [MCAD] = 1 μM + [octenoyl CoA] = 5 μM (trace 3).

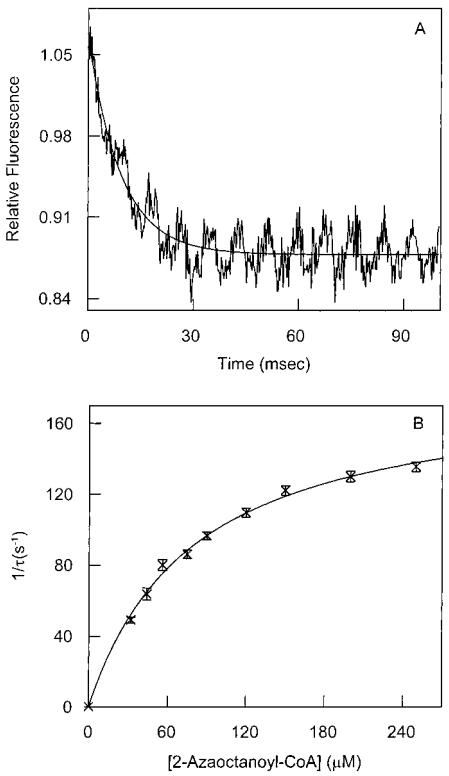

FIGURE 5: Transient kinetics for the changes in the tryptophan fluorescence of MCAD upon interaction with 2-azaoctanoyl-CoA. The excitation wavelength and cutoff filters were 295 and 335 nm, respectively. Other experimental conditions were the same as in Figure 2. Panel A shows the stopped-flow kinetic trace for the decrease in the tryptophan fluorescence of the enzyme upon binding with 2-azaoctanoyl-CoA at 5 °C. The after-mixing concentrations of MCAD and 2-azaoctanoyl-CoA were 4 and 200 μM, respectively. The solid smooth line is the best fit of the experimental data according to the single-exponential rate equation with relaxation rate constant ($1/\tau$) of 130 $\pm$ 3 s^{-1}. Panel B shows the 2-azaoctanoyl-CoA-dependent relaxation rate constant ($1/\tau$) for the enzyme−ligand interaction. The after-mixing concentration of MCAD was 4 μM. The solid smooth line is the best fit of the experimental data for the hyperbolic dependence of $1/\tau$ on 2-azaoctanoyl-CoA, with the magnitudes of $1/\tau_{max}$, $1/\tau_{min}$, and K_c being equal to 182 $\pm$ 5 s^{-1}, 0.18 $\pm$ 0.001 s^{-1}, and 79.3 $\pm$ 5.3 μM, respectively. The experimental data at zero concentration of 2-azaoctanoyl-CoA (i.e., $1/\tau_{min}$) were taken from the dissociation off-rate measurement of the enzyme−2-azaoctanoyl-CoA complex.

enzyme with 400 μM 2-azaoctanoyl-CoA (top panel) via the stopped-flow syringes at 5 °C. The solid smooth line is the best fit of the experimental data, according to the single-exponential rate equation, for the association rate constant ($1/\tau$) of 130 $\pm$ 3 s^{-1}. Note that this value is similar to the association rate constant for the binding of 2-azaoctanoyl-CoA to the enzyme (143 $\pm$ 2 s^{-1}), determined via measuring the changes in the electronic structure of the enzyme-bound FAD at 438 nm (see Figure 3A). We further investigated the effect of 2-azaoctanoyl-CoA on the magnitude of $1/\tau$ (under the pseudo-first-order condition; [E−FAD] $\ll$ [2-azaoctanoyl-CoA]), determined via the fluorescence method (Figure 5B). The solid smooth line is the best fit of the experimental data for the hyperbolic dependence of $1/\tau$ on 2-azaoctanoyl-CoA with an offset (a measure of the dissociation "off-rate" constant of the enzyme−ligand complex; see above). It should be pointed out that unlike the absorption method, we could not independently determine the dissociation "off-rate" constant of the enzyme−ligand complex by the fluorescence method. This is because the competing/displacing ligand (e.g., acetoacetyl-CoA) had more or less the same quenching property as the primary ligand, 2-azaoctanoyl-CoA or octenoyl-CoA. Hence, the increase in fluorescence due to displacement of the primary ligand was compensated by the decrease in fluorescence due to binding of the competing ligand, acetoacetyl-CoA. Therefore, no change in the fluorescence signal was found to occur during the experimental conditions of ligand dissociation from the enzyme site. Due to the above limitation, the magnitude of the dissociation "off-rate" of 2-azaoctanoyl-CoA from the enzyme site was taken from the absorption data of Figure 3B. The hyperbolic plot of Figure 5B yields the magnitudes of $1/\tau_{max}$, $1/\tau_{min}$, and K_c to be 182 $\pm$ 5 s^{-1}, 0.18 $\pm$ 0.001 s^{-1}, and 79.3 $\pm$ 5 μM, respectively. Note that the above values are similar to those determined from the changes in the electronic structure of the enzyme-bound FAD (see Figure 3C). Such a similarity attests to the fact that the changes in the electronic structure of the enzyme-bound FAD are somehow coupled to the changes in the microenvironment of the enzyme's tryptophan residues.

We previously failed to obtain the hyperbolic dependence of $1/\tau$ (the relaxation rate constant for the association of octenoyl-CoA with the enzyme, measured via the changes in the electronic structure of FAD) as a function of octenoyl-CoA concentration, due to our inability to vary the ligand concentration from subsaturating to saturating concentration regions, while maintaining the pseudo-first-order condition (*7*−*8*). Since the above limitation did not appear to pose any problem while utilizing the enzyme's tryptophan fluorescence signal, we determined the octenoyl-CoA concentration-dependent relaxation rate constant for the enzyme−ligand interaction (Figure 6). Figure 6A shows the stopped-flow transient kinetic data for the decrease in the enzyme's tryptophan fluorescence (λ_{ex} = 295 nm, cutoff filter = 335 nm) upon mixing (premixing concentrations) of 4 μM enzyme with 400 μM octenoyl-CoA at 5 °C. The solid

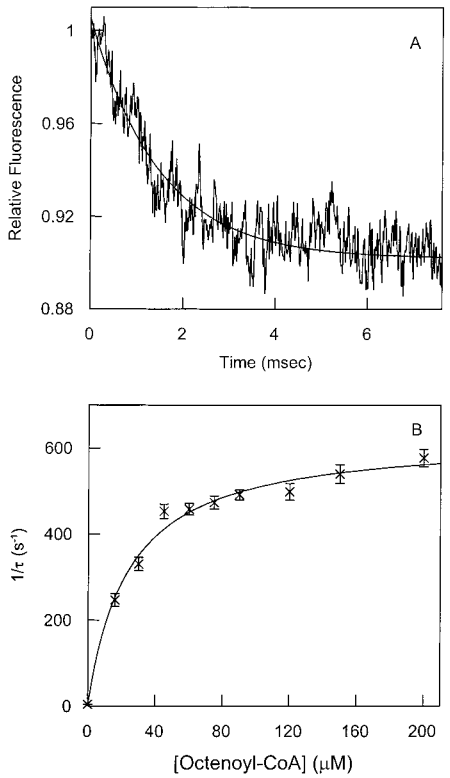

FIGURE 6: Transient kinetics for the changes in the tryptophan fluorescence of MCAD upon binding with octenoyl-CoA. Other experimental conditions were the same as in Figure 5. Panel A shows the stopped-flow kinetic trace for the changes in tryptophan fluorescence of the enzyme upon binding with octenoyl-CoA. The after-mixing concentrations of enzyme and octenoyl-CoA were 2 and 200 μM, respectively. The solid smooth line is the best fit of the experimental data according to the single-exponential rate equation for the relaxation rate constant ($1/\tau$) of 577 $\pm$ 20 s^{-1}. Panel B shows the octenoyl-CoA concentration-dependent relaxation rate constant for the enzyme−ligand interaction. The after-mixing concentration of octenoyl-CoA was 2 μM. The solid smooth line is the best fit of the experimental data for the hyperbolic dependence of $1/\tau$ on octenoyl-CoA concentration, with the magnitudes of $1/\tau_{max}$, $1/\tau_{min}$, and K_c being equal to 628 $\pm$ 20 s^{-1}, 1.0 $\pm$ 0.01 s^{-1}, and 23.6 $\pm$ 3 μM, respectively. The experimental data point at zero concentration of octenoyl-CoA (i.e., $1/\tau_{min}$) was taken from an independent dissociation "off-rate" measurement of the enzyme−octenoyl-CoA complex.

smooth line is the best fit of the experimental data, according to the single-exponential rate equation, for the association rate constant ($1/\tau$) for the binding of octenoyl-CoA, found to be 628 $\pm$ 20 s^{-1}. Note that this value is similar to the fast rate constant for the association of octenoyl-CoA with MCAD (676 $\pm$ 72 s^{-1}), determined via measuring the changes in the electronic structure of the enzyme-bound FAD (*8*). Figure 6B shows the octenoyl-CoA-dependent relaxation rate constant ($1/\tau$) for the enzyme−ligand interaction. The solid smooth line is the best fit of the experimental data for the hyperbolic dependence of $1/\tau$ on octenoyl-CoA concentrations with the magnitudes of $1/\tau_{max}$, $1/\tau_{min}$, and K_c being equal to 628 $\pm$ 20 s^{-1}, 1.0 $\pm$ 0.01 s^{-1}, and 23.6 $\pm$ 3 μM, respectively.

Dissociation Constants of the Enzyme−Ligand Complexes. To determine to what extent the αCH→NH substitution affects the overall binding constant of the enzyme−ligand complex, we undertook a comparative spectrophotometric titration for the binding of 2-azaoctanoyl-CoA and octenoyl-CoA to the oxidized form of the enzyme. The absorption

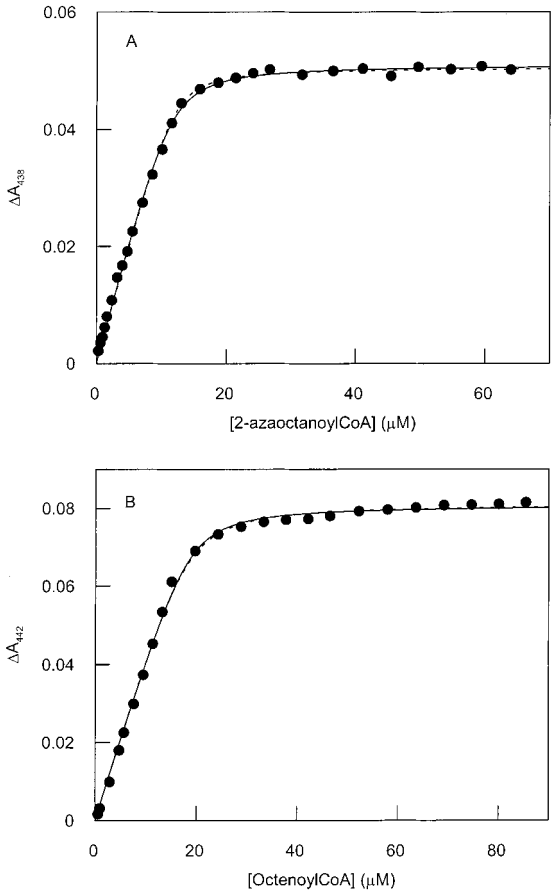

FIGURE 7: Binding isotherms for the interactions of 2-azaoctanoyl-CoA and octenoyl-CoA with MCAD. The other experimental conditions were the same as in Figure 2, except that the temperature was 25 °C. Panel A shows the titration of 18.5 μM MCAD as a function of increasing concentrations of 2-azaoctanoyl-CoA at 438 nm. The solid smooth line is the best fit of the experimental data, for a dissociation constant of 0.52 $\pm$ 0.09 μM and a stoichiometry of the enzyme−ligand complex of 0.63 $\pm$ 0.01 mol of ligand/mol of MCAD subunit. Panel B shows the titration of 18.1 μM MCAD with increasing concentrations of octenoyl-CoA at 442 nm. The solid smooth line is the best fit of the experimental data for a dissociation constant of 0.68 $\pm$ 0.16 μM and a stoichiometry of 1.03 $\pm$ 0.02 mol of octenoyl-CoA/mol of MCAD subunit. The broken lines of panels A and B are simulated lines for the dissociation constants (derived from the transient kinetic data) of the enzyme−2-azaoctanoyl-CoA and enzyme−octenoyl-CoA complexes, found to be 0.38 and 0.81 μM, respectively.

maxima for the binding of these ligands to the enzyme have been determined to be 438 and 442 nm, respectively. Figure 7A and 7B show the effects of addition of increasing concentrations of 2-azaoctanoyl-CoA and octenoyl-CoA to a fixed concentration of the enzyme solution on the absorption changes at 438 and 442 nm, respectively. The solid smooth lines are the best fit of the experimental data for a complete solution of the quadratic equation (defining a one-step enzyme−ligand interaction process) for the dissociation constants of the enzyme−2-azaoctanoyl-CoA and enzyme−octenoyl-CoA complexes, found to be 0.52 $\pm$ 0.09 and 0.68 $\pm$ 0.16 μM, respectively (*29*). Note a marked similarity between these values. These results lead to the suggestion that despite the disparity in the binding affinities of these ligands within their collision/Michaelis complexes (K_c), as well as a marked difference in their forward (k_f) and reverse (k_r) dissociation rate constants (see Discussion), the overall binding affinities of these enzyme−ligand complexes remain

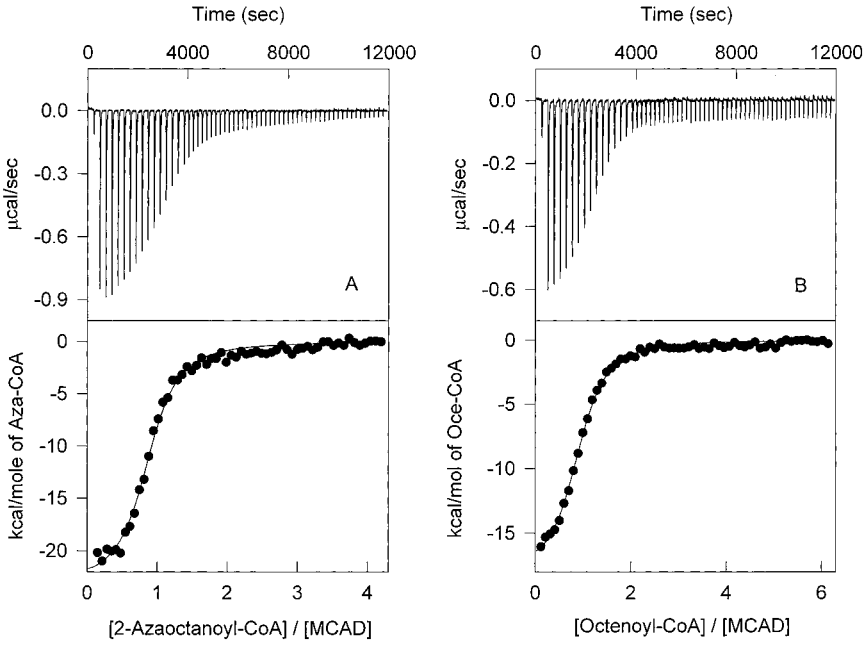

FIGURE 8: Isothermal microcalorimetric titration data for the interaction of 2-azaoctanoyl-CoA (left panels) and octenoyl-CoA (right panels) with MCAD at 25 °C. Panel A (top) shows the raw microcalorimetric data for titration of 1.8 mL of 9.87 μM MCAD with 60 injections (first injection 1 μL, subsequent injections 4 μL each) of 218 μM 2-azaoctanoyl-CoA. The area under each peak was integrated and plotted against the molar ratio of 2-azaoctanoyl-CoA to the enzyme (bottom part of panel A). The solid smooth line is the best fit of the experimental data for $n = 0.89 \pm 0.01$, $K_a = (1.96 \pm 0.16) \times 10^6$ M^{-1}, and $\Delta H° = -22.6 \pm 0.34$ kcal/mol. The experimental conditions in panel B (top) were the same as in panel A, except for the stock concentrations of MCAD and octenoyl-CoA being 10 and 288 μM, respectively. The solid smooth line in the bottom part of panel B is the best fit of the experimental data for $n = 0.95 \pm 0.01$, $K_a = (1.1 \pm 0.1) \times 10^6$ M^{-1}, and $\Delta H° = -16.9 \pm 0.17$ kcal/mol.

the same. It should be emphasized that the above differences between the binding of octenoyl-CoA and 2-azaoctanoyl-CoA to the enzyme site would have been elusive just by performing the conventional spectroscopic and/or the ligand binding experiments.

Isothermal Microcalorimetric Studies for the Binding of Ligands to MCAD. To discern the influence of α-CH→NH substitution in C_8-CoA on the thermodynamics of enzyme−ligand interactions, we undertook comparative isothermal microcalorimetric studies for the binding of 2-azaoctanoyl-CoA and octenoyl-CoA to MCAD. Figure 8 shows the isothermal microcalorimetric data for the titration of MCAD with increasing concentrations of 2-azaoctanoyl-CoA (left panel) and octenoyl-CoA (right panel) in 50 mM phosphate buffer, pH 7.6, containing 0.3 mM EDTA and 10% glycerol at 25 °C. The top panels show the raw calorimetric data. Note that the addition of each aliquot follows the emergence of a negative (exothermic) peak due to the enzyme−ligand interaction. The area under each peak serves as the measure of the amount of heat produced upon ligand binding. Note that as the titration progresses, the area under the peak becomes smaller due to increased occupancy of the enzyme site by the ligand. The bottom panels of Figure 8 show the plots of the amount of heat generated per injection as a function of the molar ratios of the ligands to the enzyme. The solid smooth line (in the left panel) is the best fit of the experimental data according to Wiseman et al. (*46*) for the stoichiometry (n), the association constant (K_a), and the standard enthalpic changes ($\Delta H°$) for the binding of 2-azaoctanoyl-CoA to the enzyme being equal to 0.89 ± 0.01 (moles of bound ligand per mole of MCAD subunit), $(1.96 \pm 0.16) \times 10^6$ M^{-1}, and -22.6 ± 0.34 kcal/mol, respectively. The corresponding parameters for the binding of octenoyl-CoA to the enzyme (the right bottom panel) were discerned to be 0.95 ± 0.01, $(1.1 \pm 0.1) \times 10^6$ M^{-1}, and -16.9 ± 0.17 kcal/mol, respectively. From these data, the dissociation constants ($K_d = 1/K_a$) of the enzyme−2-azaoctanoyl-CoA and enzyme−octenoyl-CoA complexes could be calculated to be 0.51 ± 0.04 and 0.91 ± 0.01 μM, respectively. Note that these values are similar to the corresponding K_d values of the above complexes determined via the spectrophotometric titration method (see Figure 7). However, unlike the marked similarity in the binding affinity of 2-azaoctanoyl-CoA and octenoyl-CoA to the enzyme site, the enthalpic change ($\Delta H°$) for the binding of 2-azaoctanoyl-CoA to the enzyme site is about 5.7 kcal/mol more negative than that obtained for the binding of octenoyl-CoA. Clearly, the enthalpic gain for the binding of the former ligand is compensated by the entropic loss of an equal magnitude.

DISCUSSION

Before elaborating on the effect of α-CH→NH substitution on the kinetic and thermodynamic parameters for the binding of C_8-CoA-ligands (viz., octenoyl-CoA and 2-azaoctanoyl-CoA) to MCAD, it should be emphasized that all the transient kinetic data conform to the two-step binding model (*15*) of eq 2:

$$\text{E-FAD + Ligand} \underset{K_c}{\rightleftharpoons} \underbrace{\text{E-FAD-Ligand}}_{\text{Collision complex}} \overset{k_f}{\underset{k_r}{\rightleftharpoons}} \underbrace{\text{(E-FAD-Ligand)*}}_{\text{Isomerized complex}} \quad (2)$$

According to the rapid equilibrium assumption (*31*), the formation of the enzyme−ligand collision/Michaelis complex is much faster (likely to complete within the dead time of our stopped-flow system) than the observed relaxation phase.

Table 1: Summary of the Kinetic and Thermodynamic Parameters for the Binding of 2-Azaoctanoyl-CoA and Octenoyl-CoA to MCAD

experiments	parameters	E−2-azaoctanoyl-CoA	E−octenoyl-CoA
stopped-flow absorption method	k_f (s^{-1})	205 ± 10	676 ± 72
	k_r (s^{-1})	0.18 ± 0.001	1.0 ± 0.01
	K_c (μM)	76.6 ± 7	ND
stopped-flow fluorescence method	k_f (s^{-1})	182 ± 5	628 ± 20
	k_r (s^{-1})	ND	ND
	K_c (μM)	79.3 ± 5.3	23.6 ± 3
spectrophotometric titration	K_d (μM)	0.52 ± 0.09	0.68 ± 0.16
microcalorimetric titration	$\Delta G°$ (kcal/mol)	−8.58 ± 0.07	−8.23 ± 0.08
	$\Delta H°$ (kcal/mol)	−22.6 ± 0.34	−16.9 ± 0.17
	$T\Delta S°$ (kcal/mol)	−14.0 ± 0.41	−8.66 ± 0.16

The origin of the latter lies either in changes in the electronic structure of the enzyme-bound FAD or in the enzyme's tryptophan fluorescence. For the model of eq 2, the relationship between the microscopic and observed rate constants for the enzyme−ligand interaction can be given by eq 3.

$$1/\tau = \frac{k_f[\text{ligand}]}{K_c + [\text{ligand}]} + k_r \qquad (3)$$

Equation 3 predicts a hyperbolic dependence of $1/\tau$ as a function of ligand concentration with an offset. According to eq 3, the magnitudes of the relaxation rate constant at saturating ($1/\tau_{max}$) and zero ($1/\tau_{min}$) ligand concentrations are given by $k_f + k_r$ and k_r, respectively, and the concentration of ligand required to achieve half of the maximal saturation serves as a measure of K_c. Given this, the magnitudes of k_f, k_r, and K_c for the binding of 2-azaoctanoyl-CoA to the enzyme from the absorption kinetic data of Figure 3 can be discerned to be 205 s^{-1}, 0.18 s^{-1}, and 76.6 μM, respectively. The corresponding parameters derived from the fluorescence kinetic data of Figure 5 can be discerned to be 181 s^{-1}, 0.18 s^{-1}, and 79.3 μM. Hence, irrespective of the nature of the reporter signal (i.e., the electronic structural changes of the enzyme bound FAD or the intrinsic protein fluorescence), the microscopic parameters for the binding of 2-azaoctanoyl to the enzyme are similar. A similar conclusion can be derived for the binding of octenoyl-CoA to the enzyme (see Results), with the magnitudes of k_f, k_r, and K_c being equal to 628 s^{-1}, 1 s^{-1}, and 23.6 μM, respectively. Table 1 summarizes the kinetic and thermodynamic parameters for the binding of 2-azaoctanoyl-CoA and octenoyl-CoA to MCAD.

A comparative account of the transient kinetic and thermodynamic data for the binding of octenoyl-CoA and 2-azaoctanoyl-CoA (the αCH→NH-substituted ligand) to MCAD lead to the following conclusions: (1) The overall binding affinity of octenoyl-CoA (reaction product) to the enzyme is essentially identical to that of 2-azaoctanoyl-CoA, suggesting that the latter is unlikely to serve as the transition state analogue of the enzyme. (2) The enzyme−ligand isomerization step is intimately coupled to the changes in the protein conformation, as evident by the perturbation in the microenvironment of the enzyme's tryptophan residues. (3) Whereas the intrinsic affinity of octenoyl-CoA within the enzyme−ligand collision complex ($1/K_c$) is about 3-fold higher than that for 2-azaoctanoyl-CoA, the subsequent isomerization equilibrium (k_f/k_r) is 2-fold in favor in the case of the latter as compared to the former ligand. Such a compensatory feature within the consecutive binding steps results in a near-identity of the overall binding affinity ($1/K_d$) of these ligands to the enzyme. (4) The forward (k_f) and reverse (k_r) rate constants for the isomerization step of the enzyme−octenoyl-CoA collision complex are about 3- and 6-fold higher than those determined for the enzyme−2-azaoctanoyl-CoA collision complex, respectively. The above difference is translated into a 1.6 kcal/mol higher transition state energy barrier for the isomerization of the enzyme−2-azaoctanoyl-CoA complex as compared to the enzyme−octenoyl-CoA complex. (5) The enthalpic changes ($\Delta H°$) for the binding of octenoyl-CoA to the enzyme are about 6 kcal/mol less negative (i.e., less favorable) than those obtained for the binding of 2-azaoctanoyl-CoA.

A combination of the structural and spectroscopic data for the binding of CoA-ligands to MCAD lead to the suggestion that the atomic residues in the vicinity of the thioester region of the ligands are in close proximity to the isoalloxazine ring of the enzyme-bound FAD (see Figure 1). Depending upon the type of CoA-ligands, as well as their spatial relationships to the enzyme-bound FAD, the electronic structures of the individual species are differently perturbed. For example, based on the spectroscopic, kinetic, thermodynamic, and model building studies for the binding of structurally diverse ligands to the wild-type and E376D mutant MCADs, we demonstrated that the spatial relationships between the enzyme-bound FAD and the CoA-ligands dictate, at least in part, their binding affinities to the enzyme site (*18*).

Based on the structural−functional data of MCAD catalysis (*3*, *9*, *24*), it is conceivable that the polarization of the carbonyl group of the CoA-thioesters would influence the charge distribution among the neighboring atoms. In comparison between the bound forms of octenoyl-CoA and 2-azaoctanoyl-CoA to the enzyme, it is expected that the electrostatic field at the α-position of the former ligand (having a CH group) would be different than that obtained with the latter ligand (having an NH group). Hence, for an identical chain length, the relative charge distribution at corresponding regions would influence the energetics of the enzyme−ligand interactions. Such an expectation appears to be met upon comparison of the enthalpic changes ($\Delta H°$) for the binding of these ligands to the enzyme via microcalorimetry. The experimental data of Figure 8 clearly reveal the $\Delta H°$ for the binding of 2-azaoctanoyl-CoA to the enzyme is about 5.7 kcal/mol more favorable than that obtained for the binding of octenoyl-CoA. This is presumably due to formation of an additional hydrogen bond involving the amide nitrogen of 2-azaoctanoyl-CoA and some enzyme site residue. However, since neither spectrophotometric (see Figure 7) nor the microcalorimetric (see Figure 8) titration data show any difference in the binding affinity of these ligands to the enzyme, it follows that the favorable enthalpic contribution for the binding of 2-azaoctanoyl-CoA to the enzyme (due to αCH→NH substitution) is compensated by an unfavorable (e.g., rotational, translational, and conformational) entropic contribution of an equal magnitude.

The structural data of the pig liver enzyme reveal that there are four tryptophan residues (namely, Trp-57, Trp-166, Trp-175, and Trp-317) per enzyme subunit (*24*). Of these, Trp-166 is located within 5.9 Å distance from the carbonyl carbon

of C_8-CoA, and it is slightly relocated (with respect to its position in the ligand-free form of the enzyme) upon binding of C_8-CoA. Hence, it is not surprising that the fluorescence emission of tryptophan is quenched upon binding of both octenoyl-CoA and 2-azaoctanoyl-CoA to the enzyme (Figure 4). Although we believe that the above quenching effect is primarily associated with Trp-166, at this time, we cannot rule out the involvement of other tryptophan residues in the above process. We have already created a Trp-166→Phe mutation in the enzyme to test the above possibility, and we will report our findings subsequently.

It should be emphasized that prior to this investigation, the only supporting evidence in favor of the protein conformational change during the course of ligand binding and/or catalysis was the kinetic demonstration of the isomerization of the enzyme−ligand collision complexes (*7*−*8*, *12*, *15*). In this paper, we report for the first time (to the best of our knowledge) that the transient kinetic profiles (during the course of the enzyme−ligand interactions), discerned via the electronic structural changes of the enzyme-bound FAD, precisely match with the concomitant changes in the enzyme's tryptophan fluorescence (see Figures 5 and 6). Since the latter changes originate from the ligand-induced alteration in the microenvironment of the enzyme's tryptophan residue(s), it is surmised that at least the local structure of the enzyme (in the vicinity of the ligand binding site) is changed, a feature ascribable to the ligand-induced protein conformational changes. Other investigators have arrived at the same conclusion by performing the transient kinetic studies for the binding of ligands utilizing tryptophan fluorescence as the reporter signal (*33*−*34*).

In the above context, it has been observed that any factor that alters the kinetic profiles of flavin reduction also alters the corresponding profiles of the fluorescence changes. For example, the rate of the reductive half-reaction of the enzyme (measured via the conversion of the enzyme-bound FAD to $FADH_2$) varies with the chain length of the aliphatic acyl-CoA substrates (*14*). We have recently observed that the kinetic profiles of the above reactions can be precisely mimicked by monitoring the changes in the tryptophan fluorescence (data not shown). Likewise, certain mutations (e.g., Glu-376→Gln) impair the rate of the electronic structural changes (of the enzyme-bound FAD) upon interaction with octenoyl-CoA and 2-azaoctanoyl-CoA. Such kinetic profiles are identical to those obtained by monitoring the changes in the tryptophan fluorescence, under an identical experimental condition (data not shown). These experimental data strengthen our proposition that the protein conformational changes are coupled to the changes in the ligand structures, e.g., "chemistry" or electronic structures of the FAD and/or ligands.

The experimental data presented herein reveal that the apparent association and dissociation rate constants for the binding of 2-azaoctanoyl-CoA to the enzyme are lower than those of octenoyl-CoA, suggesting that both binding and the release of the former (αCH→NH substituted) ligand are energetically unfavorable. We believe that the origin of the above difference lies in the charge distribution around the carbonyl groups of these ligands. The α-nitrogen of 2-azaoctanoyl-CoA is (relatively) electron rich during the formation of the enzyme−ligand collision complex, but it becomes electron deficient upon polarization of the carbonyl group during the isomerization step. The (apparent) binding of 2-azaoctanoyl-CoA (vis a vis octenoyl-CoA) to the enzyme site is presumably hindered due to the electrostatic repulsion by the carboxyl groups of the two active site residues, Glu-376 and Glu-99. However, the same active site groups electrostatically stabilize 2-azaoctanoyl-CoA within the enzyme site, once its carbonyl group is polarized (during the isomerization step), resulting in its impaired dissociability from the enzyme site. Such a stabilization of the enzyme−2-azaoctanoyl-CoA complex is further supported by the fact that the formation of the above complex is enthalpically more favorable as compared to that of the enzyme−octenoyl-CoA complex (see Figure 8). This is presumably due to formation of an additional hydrogen bond between the amide nitrogen of 2-azaoctanoyl-CoA and some enzyme site residue. The role of the electrostatic environment in modulating the flavin reactivity has been elaborated by other investigators (*41*−*45*).

Since the enzyme−ligand collision complexes, involving both 2-azaoctanoyl-CoA and octenoyl-CoA, are converted into their corresponding isomerized complexes, the relationship between the overall dissociation constants (K_d) and the microscopic parameters of eq 2 can be given by the relationship: $K_d = K_c k_r/k_f$. Based on the above relationship, the dissociation constants of the enzyme−2-azaoctanoyl-CoA and enzyme−octenoyl-CoA complexes can be predicted to be 0.09 and 0.031 μM (at 5 °C) from the transient kinetic data of Figures 3C and 6, respectively. As will be published subsequently, the van't Hoff enthalpies (measured via the microcalorimetric method) for the binding of 2-azaoctanoyl-CoA and octenoyl-CoA to the enzyme are −12.7 and −9.5 kcal/mol, respectively. Based on the latter parameters, the kinetically derived dissociation constants for the binding of 2-azaoctanoyl-CoA and octenoyl-CoA would be 0.35 and 0.81 μM (at 25 °C), respectively. The latter values are similar to the dissociation constants of the above complexes (at 25 °C) determined both via the spectrophotometric (0.52 ± 0.09 and 0.68 ± 0.16 μM, respectively; see Figure 7) and via the microcalorimetric (0.51 ± 0.04 and 0.91 ± 0.01 μM, respectively; see Figure 8) titration methods. The dotted lines of Figure 7 are calculated for the kinetically predicted dissociation constants of the corresponding enzyme−ligand complexes. Note a marked correspondence between the experimentally determined (solid lines) and the calculated (dotted lines) dissociation constant values. Such a similarity attests to the internal consistency of our proposed microscopic pathway for the enzyme−ligand interaction. At this point, we note that Thorpe and his collaborators reported the dissociation constants of 2-azaoctanoyl-CoA and octenoyl-CoA from pig kidney enzyme as being equal to 51 and 89 nM, respectively (*21*). We believe the discrepancy between our results and those of Thorpe's group is due to the biological origin (pig kidney versus recombinant human liver) of the enzymes. Several such discrepancies between the pig kidney and human liver enzymes have been noted in our laboratory as well as other laboratories (*8*, *18*, *22*, *30*, *40*, *41*).

However, none of the kinetic and/or thermodynamic parameters, derived from the experimental data presented in the previous section, as well as the dissociation constant data of Thorpe's group (*21*), lead to the assignment of 2-azaoctanoyl-CoA being the transition state analogue of the enzyme. This conclusion is in a direct contradiction to the proposal of Johnson et al. (*22*), on the basis of their redox potentiometric studies. These authors have assumed that the

transition state analogues shift the redox potential of the enzyme similar to the substrate/product pair, and since the magnitudes of the redox potential shift upon binding of 2-azaoctanoyl-CoA and 3-thiaoctanoyl-CoA were 65% and 20% of those obtained with octanoyl-CoA/octenoyl-CoA pair, they ascribed the 2-azaoctanoyl-CoA to be the transition state analogue.

In view of the above assignment, we must emphasize that the transition state is a kinetically derived state, and its existence is assumed to explain the rapidity of chemical reactions (*35*). Following the proposal of Pauling that the enzyme site structures must be complementary to the putative transition states of the chemical reactions (*36*), the substrate/product analogues exhibiting unusually higher binding affinities to their cognate enzymes have been customarily assigned to be the transition state analogues (*37, 38*). Invariably, the transition state analogues exhibit much higher binding affinities to their enzyme sites vis a vis their corresponding substrates and products (*38*). Since the binding affinity (cumulative or within the "collision" complex) of 2-azaoctanoyl-CoA to MCAD is either comparable to or lower than that of octenoyl-CoA (the reaction product of the enzyme), it is difficult to conceive that 2-azaoctanoyl-CoA fits in the category of the transition state analogue.

The sequence of events associated with the binding of ligands (substrate analogues) to their cognate enzymes can be as complex as those involved during their catalytic turnovers, and, thus, the complementary studies of the above processes are likely to throw light on the kinetic mechanisms of enzymes. The comparative transient kinetic studies for the binding of slightly altered ligands, presented herein, lead to the suggestion that octenoyl-CoA is preferentially stabilized within the enzyme−ligand collision/Michaelis complex, and has to overcome a smaller transition state barrier during the isomerization process as compared to 2-azaoctanoyl-CoA. Since the latter process is kinetically equivalent to the octanoyl-CoA-dependent reductive half-reaction (i.e., "chemistry") of the enzyme (*7, 12*), it appears that the introduction of a "polar" residue at the α-position destabilizes both the ground and transition state structures during the enzyme catalysis. In this regard, it should be pointed out that our previous conclusion for the coupling between the protein conformational changes and the changes in the ligand structures (involving the functionally diverse C_8-CoA-ligands) does not hold for the α-CH→NH-substituted ligand 2-azaoctanoyl-CoA (*7, 8, 12, 14*). A qualitatively similar discrepancy was noted with smaller chain length ligands (*6, 13, 15, 19*), as well as for the binding/reactivity of C_8-CoAs with the Glu-376→Asp mutant enzyme (*39*). Thus, it appears evident that although MCAD has the potential to bind structurally different types of ligands with high affinities, its active site geometry is evolved to optimize the ligand binding and/or catalysis with aliphatic medium chain ($\sim C_8$) CoA-ligands. Such a feature may be intrinsic to the functional specificities of enzymes in general.

REFERENCES

1. Beinert, H. (1963) *Enzymes, 2nd Ed. 7*, 447−466.
2. Engel, P. C. (1990) in *Chemistry and Biochemistry of Flavoenzymes* (Muller, F., Ed.) Vol. III, pp 597−655, CRC Press, Inc., London.
3. Thorpe, C., and Kim, J.-J. P. (1995) *FASEB J. 9*, 718−725.
4. Reinsch, J., Rojas, C., and McFarland, J. T. (1983) *Arch. Biochem. Biophys. 227*, 21−30.
5. Schopfer, L. M., Massey, V., Ghisla, S., and Thorpe, M. (1988) *Biochemistry 27*, 6599.
6. Johnson, J. K., and Srivastava, D. K. (1993) *Biochemistry 32*, 8004−8013.
7. Kumar, N. R., and Srivastava, D. K. (1994) *Biochemistry 33*, 8833−8841.
8. Peterson, K. L., Sergienko, E. E., Wu, Y., Kumar, N. R., Strauss, A. W., Oleson, A. E., Muhonen, W. W., Shabb, J. B., and Srivastava, D. K. (1995) *Biochemistry 34*, 14942−14953.
9. Engst, S., Vock, P., Wang, M., Kim, J. J. P., and Ghisla, S. (1999) *Biochemistry 38* 257−267.
10. Srivastava, D. K., Wang, S., and Peterson, K. L. (1997) *Biochemistry 36*, 6359−6366.
11. Lau, S. M., Powell, P., Buettner, H., Ghisla, S., and Thorpe, C. (1986) *Biochemistry 25*, 4184−4189.
12. Kumar, N. R., and Srivastava, D. K. (1995) *Biochemistry 34*, 9434−9443.
13. Johnson, J. K. (1994) Ph.D. Dissertation, North Dakota State University, Fargo, ND.
14. Kumar, N. R. (1997) Ph.D. Dissertation, North Dakota State University, Fargo, ND.
15. Johnson, J. K., Wang, Z. X., and Srivastava, D. K. (1992) *Biochemistry 31*, 10564−10575.
16. Peterson, K. L., and Srivastava, D. K. (1997) *Biochem. J. 325*, 751−760.
17. Srivastava, D. K., Kumar, N. R., and Peterson, K. L. (1995) *Biochemistry 34*, 4625−4632.
18. Srivastava, D. K., and Peterson, K. L. (1998) *Biochemisry 37*, 8446−8456.
19. Johnson, J. K., Kumar, N. R., and Srivastava, D. K. (1993) *Biochemistry 32*, 11575−11585.
20. Powell, P. J., and Thorpe, C. (1988) *Biochemistry 27*, 8022−8028.
21. Trievel, R. C., Wang, R., Anderson, V. E., and Thorpe, C. (1995) *Biochemistry 34*, 8597−8605.
22. Johnson, B. D., Mancini-Samuelson, G. J., and Stankovich, M. T. (1995) *Biochemistry 34*, 7047−7055.
23. Kim, J. J, and Wu, J. (1988) *Proc. Natl. Acad. Sci. U.S.A. 85*, 6677−6681.
24. Kim, J.-J. P., Wang, M., and Paschke, R. (1993) *Proc. Natl. Acad. Sci. U.S.A. 90*, 7523−7527.
25. Lee, H. J., Wang, M., Paschke, R., Nandy, A., Ghisla, S., and Kim, J. J. (1996) *Biochemistry 35*, 12412−12420.
26. Lehman, T. C., Hale, D. E., Bhala, A., and Thorpe, C. (1990) *Anal. Biochem. 186*, 280−284.
27. Thorpe, C., Matthews, R. G., and Williams, C. W., Jr. (1979) *Biochemistry 18*, 331−337.
28. Bernert, J. T., and Sprecher, H. (1977) *J. Biol. Chem. 252*, 6737−6744.
29. Qin, L., and Srivastava, D. K. (1998) *Biochemistry 37*, 3499−3508.
30. Peterson, K. L., Peterson, K. M., and Srivastava, D. K. (1998) *Biochemistry 37*, 12659−12671.
31. Hammes, G. G. (1982) *Enzyme Catalysis and Regulation*, Academic Press, New York.
32. Johnson, J. K., Kumar, N. R., and Srivastava, D. K. (1994) *Biochemistry 33*, 4738−4744.
33. Kubiseski, T. J., Hyndman, D. J., Morjana, N. A., and Flynn, T. G. (1992) *J. Biol. Chem. 267*, 6510−6517.
34. Christensen, U., and Molgaard, L. (1991) *FEBS Lett. 2*, 204−206.
35. Eyring, H. (1935) *Chem. Rev. 17*, 65−77.
36. Pauling, L. (1946) *Chem. Eng. News 24*, 1375−1377.
37. Wolfenden, R., and Frick, L. (1987) in *Enzyme Mechanisms* (Page, M. I., and Williams, A., Eds.) pp 97−122, Royal Society London Press, London.
38. Wolfenden, R. (1976) *Annu. Rev. Biophys. Bioeng. 5*, 271−306.
39. Peterson, K. L., Galitz, D. S., and Srivastava, D. K. (1998) *Biochemistry 37* 1697−1705.

40. Rudik, I., Bell, A., Tonge, P., and Thorpe, C. (2000) *Biochemistry 39*, 92−101.
41. Nandy, A., Kieweg, V., Krautle, F. G., Vock, P., Kuchler, B., Bross, P., Kim, J. J., Rasched, I., and Ghisla, S. (1996) *Biochemistry 35*, 12402−12411.
42. Breinlinger, E. C., Keenan, C. J., and Rotello, V. M. (1998) *J. Am. Chem. Soc. 120*, 8606−8609.
43. Zhou, Z., and Swenson, R. P. (1996) *Biochemistry 35*, 15980−15988.
44. Druhan, L. J., and Swenson, R. P. (1998) *Biochemistry 37*, 9668−9678.
45. Mancini-Samuelson, G. J., Kieweg, V., Sabaj, K. M., Ghisla, S., Stankovich, M. T. (1998) *Biochemistry 37*, 14605−14612.
46. Wiseman, T., Williston, S. Brandt, J. F., and Lin, L.-N. (1989) *Anal. Biochem. 17*, 131−137.

BI000733W